Applied Environmental Research
- RESEARCH FOR SUSTAINABLE PLANET -

Research Article

Examining the Variability in Planetary Boundary Layer Height over Thailand: Correlations with ENSO and Aerosol Optical Depth

Sirapong Sooktawee[1], Khwanruthai Renuhom[1], Siriwan Kaewket[1], Aduldech Patpai[1], Pramet Kaewmesri[2], Thongchai Kanabkaew[3], Pichnaree Lalitaporn[4,*]

[1] *Department of Climate Change and Environment, Ministry of Natural Resources and Environment, Bangkok, Thailand*
[2] *Geo-Informatics and Space Technology Development Agency (Public Organization), Ministry of Science and Technology, Bangkok, Thailand*
[3] *Occupational and Environmental Health Program, Faculty of Public Health, Thammasat University, Pathum Thani, Thailand*
[4] *Department of Environmental Engineering, Faculty of Engineering, Kasetsart University, Bangkok, Thailand*

*Corresponding Email: pichnaree.l@ku.th

Abstract

Thailand has been facing air pollution, e.g., $PM_{2.5}$, and impacts from climate phenomena, e.g., the El Niño–Southern Oscillation (ENSO). Both air pollution and climate interact with each other. Changes in the planetary boundary layer height (PBLH) can affect $PM_{2.5}$, represented by the aerosol optical depth (AOD), and are influenced by ENSO related to changes in the PBLH. The relationships among the PBLH, ENSO, and AOD were investigated via an empirical orthogonal function (EOF), which decomposes the spatiotemporal data of the PBLH into spatial patterns and corresponding time series. Correlation analysis was used to determine the relationships between the PBL variability time series and the ENSO and AOD variations in terms of interannual variability. The analysis focuses on December–February from 1991–2020 to identify dominant PBLH variability modes and their statistical relationships with ENSO and AOD. EOF analysis reveals three interesting principal components (DecPC2, JanPC3, and FebPC2) that account for 11.3–23.5% of the total PBLH variance and that exhibit spatial correlation patterns resembling ENSO-induced patterns. These modes show patterns that are consistent with the ENSO-driven influence on PBLH variations. However, the spatial correlations between the PBLH and AOD vary across Thailand. This finding indicates that AOD changes are not driven solely by ENSO. Some regions show strong PBLH-AOD correlations, whereas others exhibit weaker relationships. For example, the PBLH increases (decreases) over the northeastern region (west side) of Thailand, which is correlated with a reduction (increase) in AOD in February during the positive phase year. These findings highlight that the PBLH and ENSO alone do not fully determine the AOD changes in Thailand. Factors, such as fire emissions, monsoonal influences, and regional transport processes, play significant roles. Further studies are needed for a better understanding of the mechanism affecting air pollution to address the impacts of both air pollution and climate.

ARTICLE HISTORY

Received: 27 Oct. 2024
Accepted: 26 Feb. 2025
Published: 26 Mar. 2025

KEYWORDS

PBLH;
ENSO;
AOD;
Climate;
Thailand

Introduction

Climate change and air pollution are important issues for global, national, and local communities. Their interactions in the atmosphere are interrelated and influence each other [1–3]. The lowest part of the atmosphere, the planetary boundary layer (PBL), plays an important role in climate [4], weather [5], and air quality [6]. Southeast Asia, including Thailand, faces issues related to climate change and air quality caused by meteorological and emission influences [7]. High

concentrations of particulate matter less than 2.5 microns ($PM_{2.5}$) are crucial air pollutants in Thailand [8]. The concentration is a proportion of the mass to the air volume, which is related to the area and height. Many studies in Thailand have focused on emissions, whereas fewer have assessed climate change and climate variability [9–15]. Changes in height affect air volume, which influences the concentration of $PM_{2.5}$ in the atmosphere. Therefore, observing the variability in planetary boundary layer height (PBLH) is important for understanding its influence on suspended particles in the atmosphere and its connection to climatic phenomena.

The PBLH is directly influenced by surface conditions and extends from the ground up to a few kilometers high. The height varies with time, weather conditions, and geographic location. Turbulent mixing within this layer plays a crucial role in the redistribution of heat, moisture, and pollutants [16]. A higher PBL enhances vertical mixing, which results in the dilution of surface-level pollutants, e.g., lowering $PM_{2.5}$ levels. A deeper layer allows for better horizontal dispersion. A shallower PBLH can trap $PM_{2.5}$, resulting in elevated concentrations. $PM_{2.5}$ and the aerosol optical depth (AOD) are closely related. The AOD quantifies the extent to which aerosols prevent sunlight from passing through the atmosphere via remote sensing techniques. $PM_{2.5}$ refers to particulate matter less than 2.5 micrometers in size suspended in ambient air that can be measured by quantifying the mass of particles per unit of air volume. The AOD serves as an input for estimating $PM_{2.5}$ concentrations in the atmosphere. Higher concentrations of PM2.5 typically correlate with increased AOD, which implies that more particles in the air contribute to greater light scattering and absorption [17–19]. Therefore, PBLH is essential for understanding air quality [20].

The height of the planetary boundary layer is intricately connected to climate change and rising temperatures. The dynamics of the PBL are modified, resulting in changes in the PBLH due to variations in surface heating and atmospheric stability. Warmer conditions may increase the frequency and intensity of temperature inversions, which can lead to stagnant air conditions [4, 21]. Studies in eastern China have shown that changing sea surface temperature (SST) during El Niño events can further reduce the PBLH by varying atmospheric circulation patterns and enhancing the occurrence of inversion temperatures. Conversely, La Niña conditions typically result in higher PBLHs due to increased mixing. The interplay between the SST and PBLH can influence precipitation patterns and contribute to extreme weather events such as haze [22–23]. Nevertheless, understanding the associations among atmospheric pollution, atmospheric variability, and oceanic phenomena, e.g., ENSO, is necessary. Thus, the PBLH may serve as a critical factor linking atmospheric processes with climatic phenomena. As the climate continues to warm, the relationships among the PBLH, AOD, and ENSO become crucial for improving our understanding of climate change impacts.

Thailand is significantly affected by $PM_{2.5}$ [24] and the ENSO phenomenon [25–26]. The impacts of both may be related to the variability in the PBLH. This study aims to address the gaps in knowledge regarding these interactions in the context of Thailand. By investigating the relationships between the PBLH, AOD, and ENSO, we hope to enhance our understanding of how these factors influence air quality and climate. This research seeks to provide scientific information that can inform policymakers and the public in understanding climatic factors, such as ENSO, that affect air quality management.

Materials and methods

1) Study area

Thailand is located in the Indochina peninsula, and the neighboring countries are Myanmar, Laos, Cambodia, and Malaysia. An area from 5°N to 21°N and 97°E to 106°E (Figure 1) was selected as the domain representing Thailand for this study. In addition to the emission sources and transboundary pollution, we design a study domain in which our primary aim is to explore the PBLH variability across Thailand. The domain of this study was intentionally limited to Thailand, with the grid coordinates chosen to capture the variability of PBLH within the country. Using a larger domain, the EOF analysis would likely introduce signals from outside the country. The months of December, January, and February were selected to represent the winter season. During this time, stable atmospheric conditions, including temperature inversions, commonly dominate the region and contribute to elevated air pollution levels. This stability is related to a shallower planetary boundary layer and more confined vertical mixing, which results in more pollutant accumulation near the surface than in other seasons [27–28]. Wind circulation over the Indochina Peninsula during the winter season is influenced by the East Asian Winter Monsoon. The EAWM splits into two branches, one turning northward and the other penetrating the Indochina Peninsula. At low levels, northeast winds are dominant and blow through Vietnam, Laos, and Cambodia through Thailand [29]. Pollutants in the atmosphere are carried by winds and transported across borders from neighboring countries to the country [7]. Moreover, the variability of wind during the winter over the Indochina Peninsula is related to changes in ENSO phases [29].

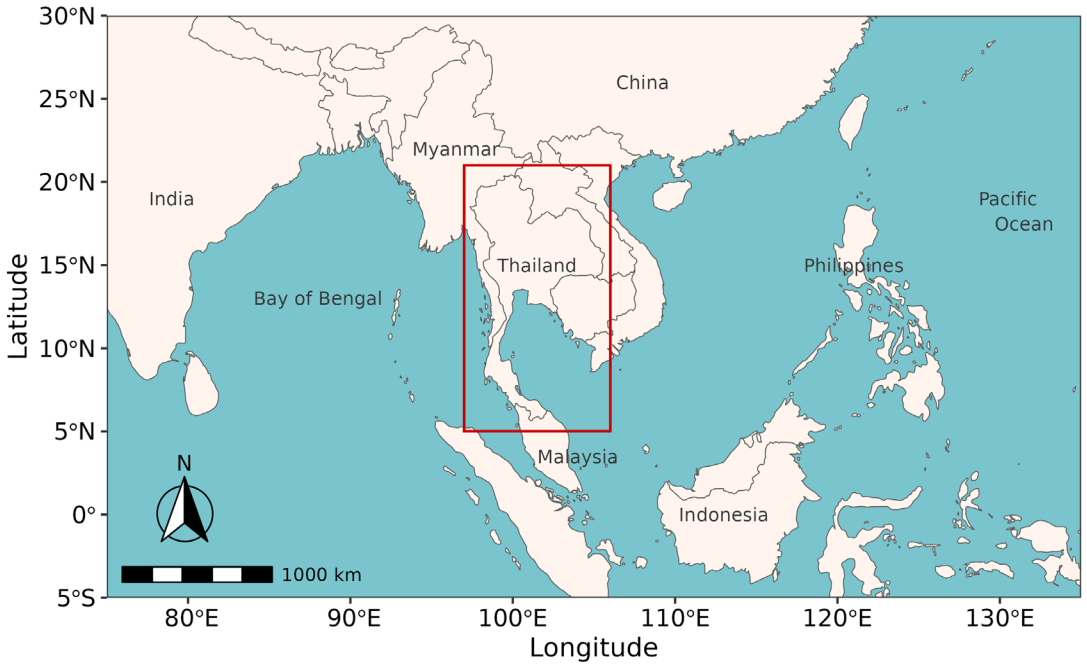

Figure 1 A study domain (red rectangle) for PBLH variability analysis over Thailand.

2) Data and methods

The data used in this study are monthly ERA5 reanalysis data and VIIRS-AOD data with 0.25° × 0.25° grid resolutions provided by the Copernicus Climate Change Service and the National Oceanic and Atmospheric Administration (NOAA), respectively. The ERA5 dataset combines observational and simulated data to provide a consistent reconstruction of past atmospheric conditions with verification of the observed data [30–31]. This makes it highly effective for analyzing historical variability. The time series of ENSO (Niño 3.4 and SOI) indices used to monitor El Niño and La Niña events in the Pacific Ocean and the DMI index used for the Indian Ocean Dipole phenomenon are also provided by NOAA. We obtained the ERA5 data from https://cds.climate.copernicus.eu/datasets. The ENSO indices and DMI indices are available at https://www.ncei.noaa.gov/access/monitoring/enso/sst and https://psl.noaa.gov/gcos_wgsp/Timeseries/DMI/, respectively. The VIIRS aerosol optical depth data are available at https://noaa-jpss.s3.amazonaws.com/index.html#SNPP/VIIRS/SNPP_VIIRS_Aerosol_Optical_Depth_Gridded_Reprocessed/. The analysis period of 1991–2020 was chosen according to the reference period suggested by the World Meteorological Organization (WMO). Notably, the AOD data have a shorter time span (2012–2020) than the other datasets do, which is a limitation of the available AOD data and our study.

The monthly PBLHs of ERA5 were separated into three space-time datasets for December, January, and February, whose anomalies were calculated before analysis via the empirical orthogonal function (EOF) to distinguish modes of variability for each month. Monthly data from several datasets, including ERA5, have been utilized for climate analysis and EOF analysis to illustrate variability [32–35]. The EOF technique has been used to decompose a continuous space-time dataset, e.g., climate data, into special modes and associated time series. The space-time data matrix $X(t,s)$, where t denotes time and where s denotes spatial location. Decomposition can be performed via the following concept:

$$X(t,s) = \sum_{k=1}^{M} c_k(t) a_k(s) \quad \text{(Eq. 1)}$$

where c_k (t) and a_k (s) are an expansion function of time and a set of functions of space. Before decomposition, the anomaly data matrix is prepared by calculating the difference between the data and climatology (mean). Next, the covariance matrix of the data, which contains p locations, is determined as follows:

$$S = \frac{1}{n} X^T X \quad \text{(Eq. 2)}$$

To obtain spatial patterns and associated time series, we compute

$$S\mathrm{u_k} = \lambda_k \mathrm{u_k}, \; k = 1, \ldots, p. \quad \text{(Eq. 3)}$$

where λ_k is the eigenvalue of the k^{th} mode and where u_k is the k^{th} eigenvector or the k^{th} EOF mode. The principal component (PC) time series can be revealed by projecting the original data on the eigenvectors as follows:

$$a_k = X u_k \quad \text{(Eq. 4)}$$

The k^{th} PC time series given by projection is associated with the k^{th} EOF mode exhibiting a spatial pattern and

can account for the variance of the k^{th} mode by using λ_k as the eigenvalue [26, 36–37].

To investigate the relationships of variability represented by the PCs to ENSO and AOD, we determine the correlation between the PCs and the corresponding indices to present which mode is related to ENSO and AOD changes. Nino3.4 is based on SST variations over the area of 5°N–5°S, 120°-170°W in the Pacific Ocean [38]. The index showed a negative relationship with the SOI [39]. Both indices have been used to characterize El Nino and La Nina events in the Pacific Ocean [38], whereas the dipole mode index (DMI), which represents the Indian Ocean Dipole (IOD) phenomenon, has been used to present the interannual climate variability in terms of the sea surface temperature (SST) in the Indian Ocean [40]. The ENSO, IOD, and AOD data were used to observe their correlations with the variabilities in the PBLH (PCs).

The correlation coefficients of 0, < 0.2, 0.2-0.4, 0.4-0.7, 0.7-0.9, 0.9-1.0, and 1 imply no relationship, almost negligible relationship, small relationship, substantial relationship, marked relationship, very dependable relationship, and perfect relationship, respectively, and refer to both positive and negative directions [41]. The correlations of PCs with ENSO and IOD, which are strongly related or greater than that relationship, are then used to interpret the correlation map of PC with AOD. In brief, the analysis can be summarized as follows: 1) Conduct EOF analysis to obtain spatial patterns (EOF modes) and the PC time series (representing variability). 2) Determine the correlation between the PC time series and the Nino3.4 and DMI indices to identify possible relationships. 3) Identify the PCs that correlate significantly with the indices and present their spatial patterns along with their corresponding PCs. 4) Compute the correlation coefficients between the selected PCs and the SST for each ocean grid cell, leading to a correlation map showing the relationship between the PBLH variability (PCs) and the SST. 5) Perform a similar analysis to step 4 but use AOD data instead of SST data, which aims to reveal the relationship between PBLH variability (PCs) and AOD. This will present the association of PBLH variability related to SST phenomena and AOD. The challenge of this study is the use of EOF analysis in view of climate and air quality to identify interesting spatial and temporal modes of PBLH. However, these limitations may not fully capture localized air quality or specific emission sources.

Results and discussion

1) PBL variability and correlations with ENSO

For December, the first, second, and third modes explain 37.7%, 23.5%, and 7.1% of the total variance, respectively. The contributions of the first, second, and third modes for January are 29.8%, 19.0%, and 11.3%, respectively, and the eigenvalues for February are 30%, 17.4%, and 13.7% for the first, second, and third modes, respectively (as shown in the supplementary material). Both the PCs and climatic indices (SOI, Nino3.4, and DMI) were calculated to determine their correlation coefficients, as shown in Figure 2. The PC2 variation during the December (DecPC2) period was significantly correlated with the SOI, Nino3.4, and DMI, with values of 0.5, –0.59, and –0.46, respectively. However, a statistically significant relationship between DecPC1 and DecPC3 and the indices did not appear. In addition to December, significant correlations of JanPC3 with the SOI, Nino3.4, and DMI for January were observed: 0.55, –0.54, and no significant correlations, respectively. Finally, we observed significant correlations between the FebPC1 and ENSO indices for the February period, with values of –0.5 and 0.47, and the correlations between the FebPC2 and ENSO indices were 0.36 and –0.48, respectively. The relationships between the three FebPCs and the DMI were not significantly correlated. There is no correlation between FebPC1 and FebPC2 because of the orthogonal property given by EOF analysis. These significant relationships are therefore interesting for exploring and exhibiting spatial correlations with SST only in the Pacific Ocean and with AOD over Thailand.

Before elaborating on the relationships between the variabilities in SST and AOD, we explain the characteristics of the significant modes. In December, EOF2 (DecEOF2) has a negative loading over southern Thailand, a light negative loading over northern Thailand, and a positive loading over northeastern Thailand. This implies a rise in DecPC2, resulting in a decrease (increase) in the PBLH in southern (northeastern) Thailand, and vice versa for a decrease in the DecPC2 amplitude. However, in the northern and central parts of Thailand, the EOF loading is quite neutral, which means that the change in the PBLH is small across these areas. The EOF3 of January (JanEOF3) is quite similar to that of DecEOF2, but the positive loading area expands from northeastern to some central and northern parts of Thailand. In February, EOF1 (FebEOF1) has a mostly positive loading over Thailand, except for the area above 18°N, which has a light negative loading. The 2nd mode (FebEOF2) is comparable to the patterns of DecEOF2 and JanEOF3. The negative loading over southern Thailand in FebEOF2 is greater than that in JanEOF3 and expands to cover western and northern Thailand (Figure 3 (d)). The resemblance between these three modes (DecEOF2, JanEOF3, and FebEOF2) could result from the same factor, whereas FebEOF1 would differ from the others.

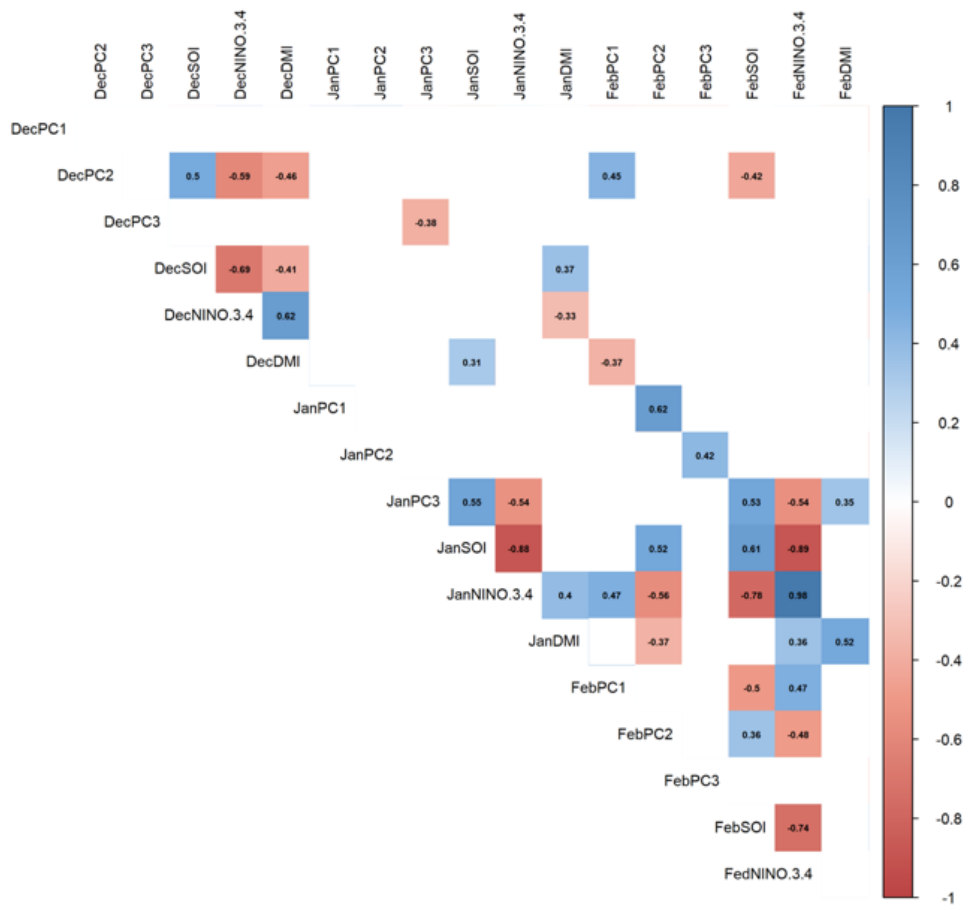

Figure 2 Significant correlations between PCs and indices ($p < 0.05$).

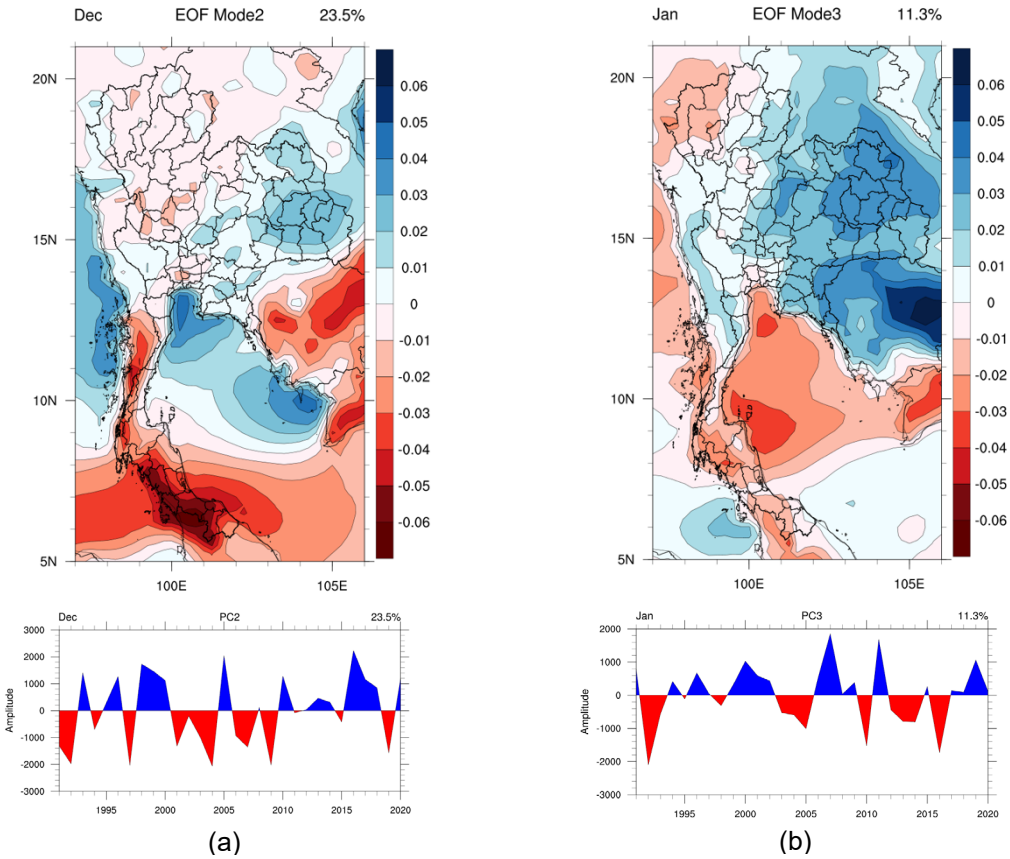

(a) (b)

Figure 3 Interesting EOFs of PBL variability and corresponding PCs.

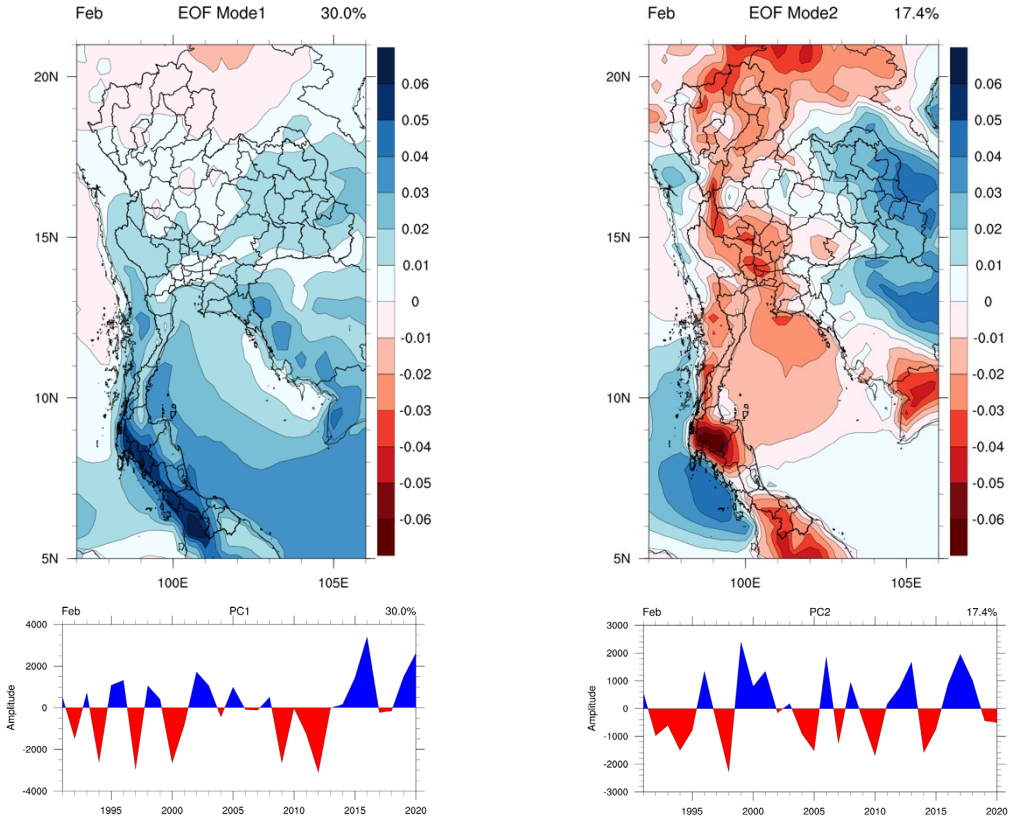

Figure 3 Interesting EOFs of PBL variability and corresponding PCs (*continued*).

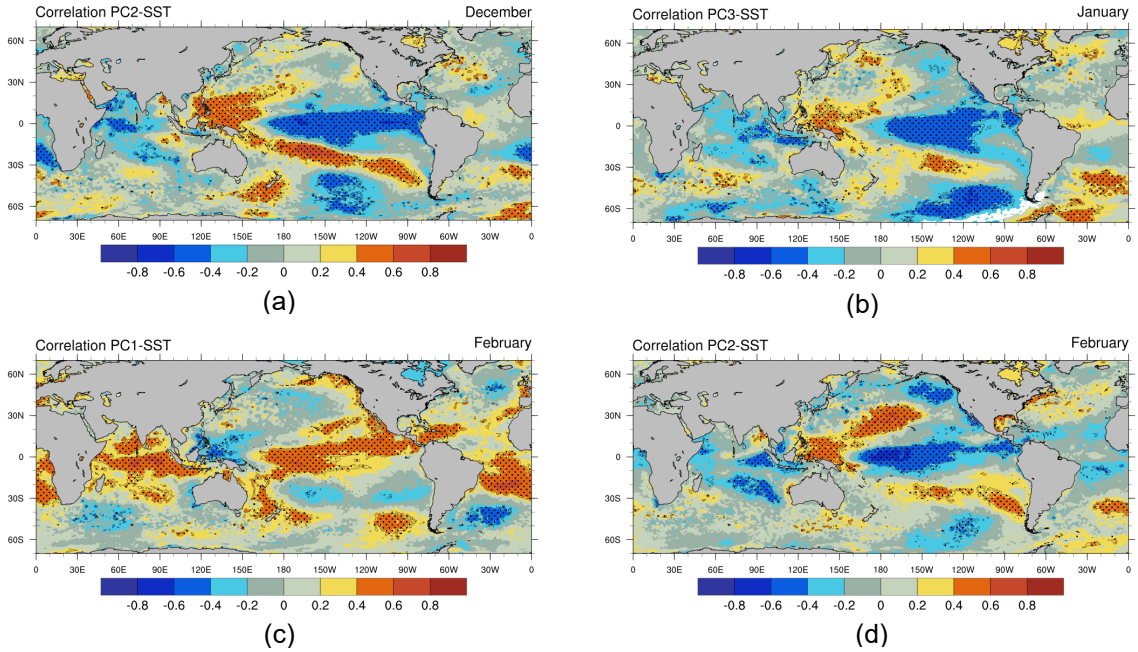

Figure 4 Correlation maps of PCs to the SST.

Four PCs were used to determine the spatial correlation pattern of sea surface temperature anomalies. The correlation maps of PCs with respect to SST, with the exception of PC1 in February, reveal that the spatial patterns are quite similar. They (Figures 4 (a), (b), and (d) show a substantial negative relationship over the Central East Pacific Ocean and a cold tongue-like appearance, whereas PC1 in February (FebPC1) shows the opposite pattern. Figure 4c shows a positive substantial correlation, which is comparable to the warm phase in the central Pacific Ocean. These findings are consistent with the substantial relationships between the PCs and ENSO indices mentioned previously.

This result revealed the teleconnection of PBLH variability with ENSO. In addition to the influence of ENSO on precipitation, temperature, and wind circulation

in Thailand [26, 29], it can also influence the change in PBLH, as reported by another study [42].

2) Correlation with AOD

The relationship between PBLH variability and AOD was observed to present a magnitude response that can imply a change in $PM_{2.5}$ related to PBLH variability. In December, Figure 5 (a) reveals substantial negative relationships over the North, West, and Central parts of Thailand, whereas a small negative relationship occurs in the Northeast Region. A negative correlation means that increasing the PC amplitude is related to reducing the AOD. However, in this southern region, the correlations between DecPC2 and AOD have a positive relationship with a substantial relationship. The DecPC2-AOD relationship is opposite to that in other areas. Therefore, the deepening and shallowing of the PBLH during the positive phase year over the northeastern part and southern part was related to a small reduction and increase in the AOD, respectively. The next pattern in January, the northeastern region, showed substantial negative relationships with the JanPC3 and AOD (Figure 5 (b)), that is, when JanPC3 increases, it cooccurs with the reduction in AOD. As mentioned previously, JanEOF3 (Figure 3 (b)) shows positive loading over the northeastern region during positive phase (positive JanPC3) years, which implies that the height increases over this region during this period, and vice versa for negative phase years. The area on the west side (< 100°E) shows a positive correlation (Figure 3 (b)), which is the opposite characteristic of the northeastern region. The increase in AOD at the western site is related to the increase in JanPC3, which corresponds to a negligible change in the PBLH in the western part of Thailand and a substantial PBLH reduction in the southern part of Thailand. During February, the correlation of FebPC1 with AOD shows almost no relationship and an almost negligible relationship (Figure 5 (c)), and Figure 5 (d) shows a similar pattern in January. Therefore, the relationship and behavior of the PBLH during February affect the AOD, similar to the interrelationship between the PBLH and AOD in January. These results agree with those of a previous study that revealed that the PBLH in winter is shallower than that in other seasons and is positively related to surface temperature [43]. Importantly, the relationship is not always statistically significant and does not consistently follow a negative relationship. The AOD and $PM_{2.5}$ concentrations are affected by multiple factors beyond the PBLH, such as emissions, wind, synoptic-scale weather, and atmospheric stability. In cases where strong winds prevail and aerosol concentrations are low, the PBLH may not be the primary driver of pollution variability, resulting in weak or negligible correlations [44]. A reduction in the PBLH cooccurs with a decrease in the wind speed, resulting in a decrease in the atmospheric ventilation capacity [43]. Therefore, both a reduction in the PBLH and a decrease in the wind speed result in a decrease in the ventilation coefficient, which enhances pollution trapping within the PBL. Moreover, wind circulation over Thailand is different and depends on the geographical features of each region. The magnitude of the wind speed over Thailand is also related to the strength of the winter monsoon, which is related to the ENSO [29]. Pollution trapping in the atmosphere over Thailand during the winter season is related to variabilities in the PBLH and wind speed, resulting in changes in ventilation capacity, which are influenced by large-scale phenomena, such as the winter monsoon and ENSO.

These results indicate that there are interesting variabilities related to variations in ENSO and AOD during December, January, and February, which are DecPC2, JanPC3, and FebPC2, respectively. They account for 23.5%, 11.3%, and 17.4% of the variance for December, January, and February, respectively. The corresponding EOF reveals the spatial pattern of the loading of PBLH changes for Thailand in various areas. The correlations between the three PCs and the Nino3.4 index show substantial relationships, and the correlation maps of PCs to SST are similar to those of the ENSO pattern. For example, in February, the PBLH increases (decreases) over the northeastern region (west side) of Thailand during positive phase years, which cooccurs with SST cooling in the central Pacific Ocean (La Nina like). On the other hand, this characteristic of interrelationships exhibited opposite patterns in the negative phase years, which would correlate with El Nino. The variation in PC during February also correlates with spatial AOD changes in different patterns. PBLH increases (decreases) over the northeastern region (west side) of Thailand, which is correlated with a reduction (increase) in AOD during positive phase years. Notably, the variation accounts for approximately 20% of the variance. Thus, PBLH variability, ENSO, and AOD variation are interrelated, which may result in $PM_{2.5}$ changes caused by the influence of PBLH variability of approximately 20%. However, more analyses and studies are needed to understand and explain the complex mechanism by which climatic factors affect changes in $PM_{2.5}$ in Thailand.

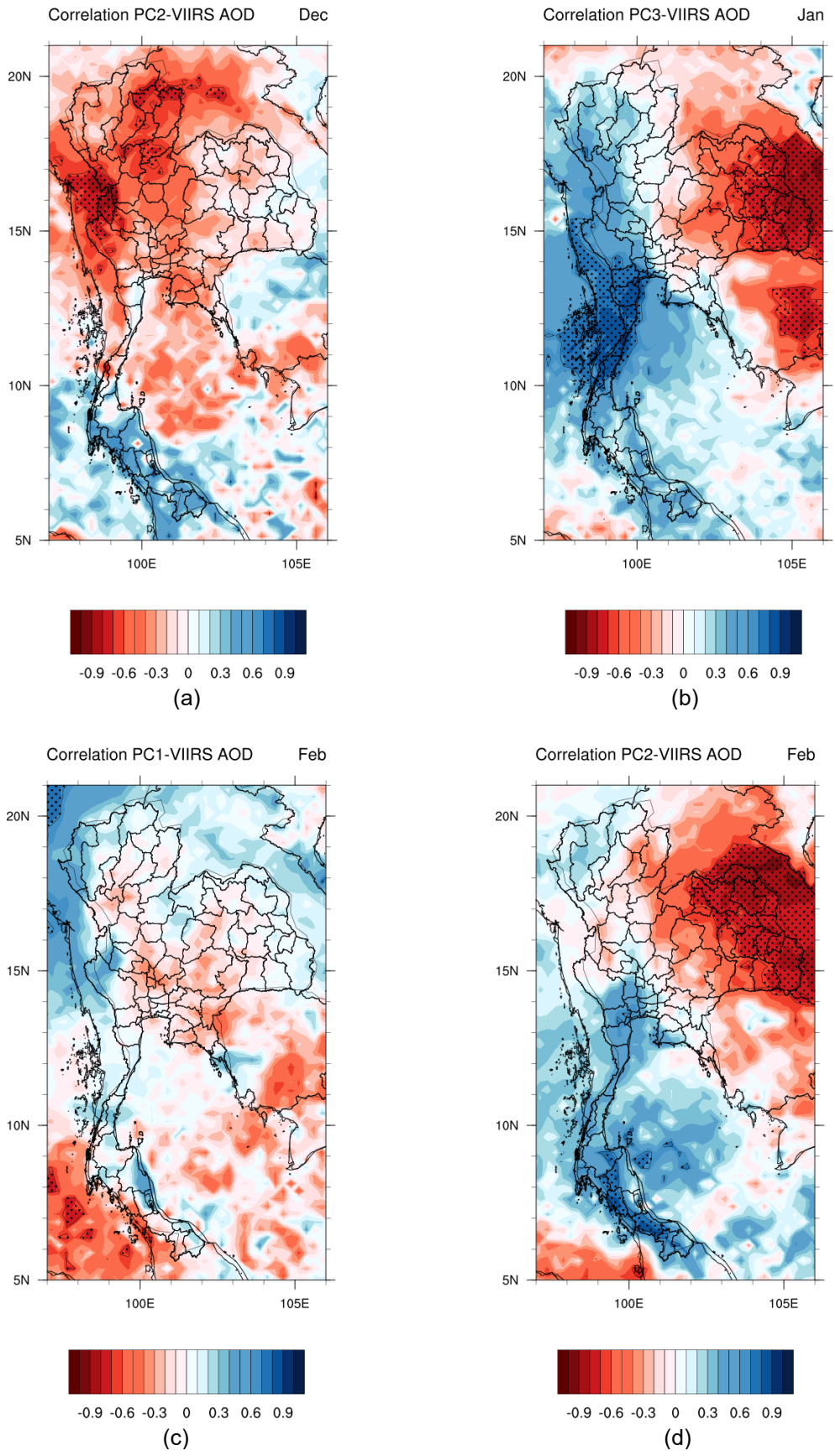

Figure 5 Correlation maps of PCs to AOD.

Conclusions

Understanding the relationships among atmospheric processes, climate variability, and air pollution is crucial for addressing Thailand's severe air pollution problems, e.g., $PM_{2.5}$. This study investigates the linkages among PBLH variability, AOD, and ENSO, highlighting how PBLH variability is related to ENSO and AOD, which represent $PM_{2.5}$. Our EOF analysis identifies three significant PBLH

variability modes, consisting of the EOF spatial pattern and PC time series, during winter (December, January, and February). We found interesting temporal variation across a variety of PC time series. DecPC2, JanPC3, and FebPC2 explained 23.5%, 11.3%, and 17.4% of the variance, respectively. These modes exhibit significant correlations with ENSO and AOD. These findings indicate that large-scale climate phenomena are associated with changes in the PBLH and affect aerosol loading over Thailand. However, other PBLH modes show no significant correlation with ENSO. Our findings imply that only 11.3%–23.5% of PBLH variability can be directly attributed to ENSO-related factors and influences on $PM_{2.5}$, as represented by the AOD. The results reveal statistically significant relationships between the PBLH and the ENSO and AOD. However, not all PBLH modes are ENSO-driven and suggest that the PBLH and ENSO are not the sole drivers of $PM_{2.5}$ variability over Thailand.

The spatial patterns of the PBLH-AOD relationships vary across different regions of Thailand in association with ENSO. Therefore, multiple factors regulate air pollution beyond ENSO phenomena. While some areas exhibit stronger correlations between PBLH and AOD, others show weaker associations, possibly due to weather conditions, emissions from sources, and atmospheric transport mechanisms. This study has limitations that should be addressed in future research. First, our analysis does not explicitly account for the role of biomass burning and fire hotspots, which are perhaps related to the leading EOF mode during the dry season. The inclusion of fire hotspot data would help distinguish between ENSO-induced variability and direct emissions from anthropogenic or natural sources. Second, the study does not assess the impact of large-scale atmospheric circulation patterns, such as the Asian winter monsoon. This may modulate the PBLH and pollutant dispersion at a broader scale. Investigating these mechanisms would enhance our understanding of how regional climate variability influences air quality.

In summary, our study demonstrates that ENSO has a measurable impact on PBLH variability over Thailand and influences AOD, which represents PM2.5 concentrations. However, the influence of ENSO is not absolute, as only a portion of the total variance in PBLH variability is related to AOD. The findings emphasize the need for continued research incorporating additional climate variability, atmospheric processes, emission source activity, and inter- and intra-annual variation analyses to better understand and mitigate air pollution in Thailand.

Acknowledgements

This study is part of the work conducted under project ID 4710006, funded by the Fundamental Fund (FF). It was also supported by: 1) the Department of Climate Change and Environment (DCCE), Ministry of Natural Resources and Environment, Thailand; 2) the Thailand Science Research and Innovation (TSRI); and 3) the National Science, Research and Innovation Fund (NSRF).

References

[1] Ruchiraset, A., Tantrakarnapa, K. Association of climate factors and air pollutants with pneumonia incidence in Lampang province, Thailand: Findings from a 12-year longitudinal study. International Journal of Environmental Health Research, 2022, 32, 691–700.

[2] Ramanathan, V., Feng, Y. Air pollution, greenhouse gases and climate change: Global and regional perspectives. Atmospheric Environment, 2009, 43, 37–50.

[3] Im, U., Geels, C., Hanninen, R., Kukkonen, J., Rao, S., Ruuhela, R., …, Aunan, K. Reviewing the links and feedbacks between climate change and air pollution in Europe. Frontiers in Environmental Science, 2022, 10, 954045.

[4] Esau, I., Zilitinkevich, S. On the role of the planetary boundary layer depth in the climate system. Advances in Science and Research, 2010, 4, 63–69.

[5] Allabakash, S., Lim, S. Climatology of planetary boundary layer height-controlling meteorological parameters over the Korean Peninsula. Remote Sensing, 2020, 12, 2571.

[6] Duc, H.N., Rahman, M.M., Trieu, T., Azzi, M., Riley, M., Koh, T., …, Kirkwood, J. Study of planetary boundary layer, air pollution, air quality models and aerosol transport using ceilometers in New South Wales (NSW), Australia. Atmosphere, 2022, 13, 176.

[7] Verma, R.L., Oanh, N.T.K., Winijkul, E., Huy, L.N., Armart, I.P., Laowagul, W., …, Patdu, M.K. Air quality management status and needs of countries in South Asia and Southeast Asia. APN Science Bulletin, 2023, 13, 130–152.

[8] Sooktawee, S., Kanchanasuta, S., Bunplod, N. Assessment of 24-h moving average PM2.5 concentrations in Bangkok, Thailand against WHO guidelines. Sustainable Environment Research, 2023, 33, 3.

[9] ChooChuay, C., Pongpiachan, S., Tipmanee, D., Suttinun, O., Deelaman, W., Wang, Q…, Cao, J. Impacts of PM2.5 sources on variations in particulate chemical compounds in ambient air of Bangkok, Thailand. Atmospheric Pollution Research, 2020, 11, 1657–1667.

[10] Sirithian, D., Thanatrakolsri, P. Relationships between meteorological and particulate matter concentrations ($PM_{2.5}$ and PM_{10}) during the haze period in urban and rural areas, Northern Thailand. Air, Soil and Water Research, 2022, 15, 1–15.

[11] Chirasophon, S., Pochanart, P. The long-term characteristics of PM_{10} and $PM_{2.5}$ in Bangkok, Thailand. Asian Journal of Atmospheric Environment, 2020, 14, 73–83.

[12] Thongsame, W., Henze, D.K., Kumar, R., Barth, M., Pfister, G. Evaluation of WRF-Chem $PM_{2.5}$ simulations in Thailand with different Anthropogenic and biomass-burning emissions. Atmospheric Environment: X, 2024, 23, 100282.

[13] Wimolwattanapun, W., Hopke, P.K., Pongkiatkul, P. Source apportionment and potential source locations of $PM_{2.5}$ and $PM_{2.5–10}$ at residential sites in metropolitan Bangkok. Atmospheric Pollution Research, 2011, 2, 172–181.

[14] Amnuaylojaroen, T., Surapipith, V., Macatangay, R.C. Projection of the near-future $PM_{2.5}$ in Northern Peninsular Southeast Asia under RCP8.5. Atmosphere, 2022, 13, 305.

[15] Kanchanasuta, S., Sooktawee, S., Patpai, A., Vatanasomboon, P. Temporal variations and potential source areas of fine particulate matter in Bangkok, Thailand. Air, Soil and Water Research, 2020, 13, 1–10.

[16] Li, Z., Guo, J., Ding, A., Liao, H., Liu, J., Sun, Y., …, Zhu, B. Aerosol and boundary-layer interactions and impact on air quality. National Science Review, 2017, 4, 810–833.

[17] Ma, Z., Dey, S., Christopher, S., Liu, R., Bi, J., Balyan, P., Liu, Y. A review of statistical methods used for developing large-scale and long-term PM2.5 models from satellite data. Remote Sensing of Environment, 2022, 269, 112827.

[18] Hoff, R.M., Christopher, S.A. Remote sensing of particulate pollution from space: Have we reached the promised land? Journal of the Air & Waste Management Association, 2009, 59, 645–675.

[19] Punpukdee, P., Winijkul, E., Kyaw, P.P., Virdis, S.G.P., Xue, W., Nguyen, T.P.L. Estimation of hourly one square kilometer fine particulate matter concentration over Thailand using aerosol optical depth. Frontiers in Environmental Science, 2024, 11, 1303152.

[20] Kulmala, M., Kokkonen, T., Ezhova, E., Baklanov, A., Mahura, A., Mammarella, I., …, Petäjä, T. Aerosols, clusters, greenhouse gases, trace gases, and boundary-layer dynamics: On feedbacks and interactions. Boundary-Layer Meteorology, 2023, 186, 475–503.

[21] Li, X., Hu, X.-M., Ma, Y., Wang, Y., Li, L., Zhao, Z. Impact of planetary boundary layer structure on the formation and evolution of air-pollution episodes in Shenyang, Northeast China. Atmospheric Environment, 2019, 214, 116850.

[22] Bai, D., Liu, L., Dong, Z., Ma, K., Huo, Y. Variations and possible causes of the December PM2.5 in Eastern China during 2000–2020. Frontiers in Environmental Science, 2023, 11, 1134940.

[23] Wang, J., Liu, Y., Ding, Y. On the connection between interannual variations of winter haze frequency over Beijing and different ENSO flavors. Science of the Total Environment, 2020, 740, 140109.

[24] Hassan Bran, S., Macatangay, R., Chotamonsak, C., Chantara, S., Surapipith, V. Understanding the seasonal dynamics of surface $PM_{2.5}$ mass distribution and source contributions over Thailand. Atmospheric Environment, 2024, 331, 120613.

[25] Sooktawee, S., Humphries, U., Patpai, A., Kongsong, R., Boonyapitak, S., Piemyai, N. Visualization and interpretation of PM_{10} monitoring data related to causes of haze episodes in Northern Thailand. Applied Environmental Research, 2015, 37, 33–48.

[26] Kirtphaiboon, S., Wongwises, P., Limsakul, A., Sooktawee, S., Humphries, U. Rainfall variability over Thailand related to the El Niño-Southern Oscillation (ENSO). Journal of Sustainable Energy & Environment, 2014, 5, 37–42.

[27] Kim Oanh, N.T., Upadhyay, N., Zhuang, Y.-H., Hao, Z.-P., Murthy, D.V.S., Lestari, P., …, Dung, N.T. Particulate air pollution in six Asian cities: Spatial and temporal distributions, and associated sources. Atmospheric Environment, 2006, 40, 3367–3380.

[28] Phung Ngoc, B.A., Delbarre, H., Deboudt, K., Dieudonné, E., Nguyen Tran, D., Le Thanh, S., …, Ravetta, F. Key factors explaining severe air pollution episodes in Hanoi during 2019 winter season. Atmospheric Pollution Research, 2021, 12, 101068.

[29] Sooktawee, S., Humphries, U., Limsakul, A., Wongwises, P. Spatio-temporal variability of winter monsoon over the Indochina Peninsula. Atmosphere, 2014, 5, 101–121.

[30] Hersbach, H., Bell, B., Berrisford, P., Hirahara, S., Horányi, A., Muñoz-Sabater, J., …, Thépaut J. The ERA5 global reanalysis. Quarterly Journal of the Royal Meteorological Society, 2020, 146, 1999–2049.

[31] Guo, J., Zhang, J., Yang, K., Liao, H., Zhang, S., Huang, K., …, Xu, X. Investigation of near-global daytime boundary layer height using high-resolution radiosondes: First results and comparison with ERA5, MERRA-2, JRA-55, and NCEP-2 reanalyses. Atmospheric Chemistry and Physics, 2021, 21,17079–17097.

[32] Ziemke, J.R., Chandra, S., Bucsela, E.J., Joiner, J., Liu, X., Zhang, L., Li, J. Evaluation of global tropospheric ozone from the OMI and TES satellite instruments: Trends and seasonal variations. Atmospheric Environment, 2013, 70, 73–83.

[33] Huang, X., Wei, J., Zhuang, J., Sun, Z., Zhang, T., Xie, Y., …, Yang, X. Impact of anthropogenic and natural emissions on air quality in the Yangtze River Delta, China. Environmental Science & Technology, 2016, 50, 6551–6559.

[34] Dey, S., Di Girolamo, L., Markowicz, K.M., Chudamani, S. Evaluation of aerosol optical depth retrieved from MODIS over South Asia during the monsoon season. Journal of Geophysical Research: Atmospheres, 2007, 112, D22202.

[35] Mahapatra, P., Behera, S.N., Pisharoty, P., Ray, R., Patra, P., Subramaniam, V., …, Rathi, S.K. Meteorological parameters and pollution trends in Northern India. Environmental Pollution, 2017, 226, 318–329.

[36] Hannachi A., Jolliffe I.T., Stephenson D.B. Empirical orthogonal functions and related techniques in atmospheric science: A review. International Journal of Climatology, 2007, 27, 1119–1152.

[37] Hannachi A. Regularised empirical orthogonal functions. Tellus A: Dynamic Meteorology and Oceanography, 2016, 68, 31723.

[38] Trenberth K.E. The Definition of El Niño. Bulletin of the American Meteorological Society, 1997, 78, 2771–2777.

[39] Trenberth K.E., Hoar T.J. The 1990–1995 El Niño-Southern Oscillation Event: Longest on Record. Geophysical Research Letters, 1996, 23, 57–60.

[40] Saji N.H., Goswami B.N., Vinayachandran P.N., Yamagata T. A dipole mode in the tropical Indian Ocean. Nature, 1999, 401, 360–363.

[41] Guilford J.P. Fundamental statistics in Psychology and Education. 1st edition. London: McGraw-Hill, 1942, 218–219

[42] Carneiro R.G., Fisch G. Observational analysis of the daily cycle of the planetary boundary layer in the central Amazon during a non-El Niño year and El Niño year (GoAmazon project 2014/5). Atmospheric Chemistry and Physics, 2020, 20, 5547–5558.

[43] Tursumbayeva M., Kerimray A., Karaca F., Permadi D.A. Planetary Boundary Layer and its Relationship with PM2.5 Concentrations in Almaty, Kazakhstan. Aerosol and Air Quality Research, 2022, 22, 210294.

[44] Su T., Li Z., Kahn R. Relationships between the planetary boundary layer height and surface pollutants derived from lidar observations over China: regional pattern and influencing factors. Atmospheric Chemistry and Physics, 2018, 18, 15921–15935.